Investigation of Seawater Intrusion in the Nile Delta Aquifer, Egypt

Asaad M. Armanuos[1], Mona Gamal Eldin Ibrahim[2], Abdelazim Negm[3], Jiro Takemura[4] and Chihiro Yoshimura[5], and Wael Elham Mahmod[6]

[1] Assistant Professor, Irrigation and Hydraulics Engineering Department, Faculty of Engineering, Tanta University, Tanta, Egypt, Email:asaad.matter@f-eng.tanta.edu.eg
[2] Dean of School of Energy Resources, Environmental and Chemical & Petrochemical Engineering, Egypt-Japan University of Science and Technology, New Borg El Arab City, Alexanderia, Egypt, Email: mona.gamal@ejust.edu.eg
[3]Prof of hydraulics, Faculty of Engineering, Zagazig University, Zagazig, Egypt, Email:amnegm@zu.edu.eg
[4]Dr. of Eng., Associate Professor, Dept. of Civil Engineering, Tokyo Institute of Technology(2-12-1 Oookayama, Meguro, Tokyo 152-8552, Japan), Email: jtakemur@cv.titech.ac.jp
[5]Dr. of Eng., Associate Professor, Dept. of Civil Engineering, Tokyo Institute of Technology
(2-12-1Oookayama, Meguro, Tokyo 152-0033, Japan, Email: yoshimura.c.aa@m.titech.ac.jp
[6]Civil Engineering Department, Faculty of Engineering, Assiut University, 71515, Assiut, Egypt, Email: dpp2006@aun.edu.eg

***Abstract*-In coastal groundwater aquifer, seawater intrusion is seen as a significant issue. Increasing the groundwater pumping rate enhances seawater intrusion into groundwater in the coastal aquifers. In Egypt, the Nile Delta aquifer (NDA) is extremely vulnerable to Mediterranean Sea seawater intrusion. The study's major goal was to create a three-dimensional groundwater model that included main branches of the irrigation system and their groundwater recharges into the NDA. The NDA model was built by using the SEAWAT program. The model validation was achieved by comparing its results with the observation data and results from previous models. Three scenarios were proposed considering: 1) sea level rise, 2) changes in the rate of groundwater abstraction, and 3) a combination of the conditions of the two previous scenarios' conditions. A rise in Mediterranean Sea levels by 25, 50, 75 and 100 cm caused additional saltwater intrusion to distances of 5.11 km, 7.10, 7.62 and 8.2 km, respectively. Moreover, in comparison to the base situation, a decrease in the lower boundary's groundwater head by 25, 50, 75 and 100 cm caused the saltwater to advance further inland to distances of 5.30, 5.47, 5.52 and 5.75 km, respectively. The third scenario proved to be the worst case, in which saltwater intrusion increased to a distance of 7.22, 7.73, 8.20 and 10.20 km, respectively. Compared with previous model studies, the results showed that saltwater intrusion length decreases by 4.0 km after including all branches of the irrigation network.**

Keywords: Groundwater, Nile Delta Aquifer, Climate Change, Groundwater Pumping, Sea Level Rise.

I. INTRODUCTION

In numerous areas of the world, groundwater in the coastal aquifers is a significant supply of freshwater, particularly in dry and semi-arid regions where rainfall is low and surface fresh water bodies are scarce. Groundwater resources are being used in arid and semi-arid regions as coastal zones grow and urbanize (Abd-Elhamid 2010). Excessive groundwater abstraction has a considerable consequence on saline intrusion in coastal aquifers, as the fresh groundwater outflow to the sea reduces, causing saline water to enter inland into the aquifer (Abd-Elhamid 2010). Numerous studies have utilized different numerical methods to determine the degree of saltwater intrusion into the NDA. The sharp interface method had already been used in earlier investigations, while recent studies have been established on the variable density and dispersion zone approaches. Wilson et al. (1979), Amer and Farid (1981), Farid (1980, 1985) and Sakr et al. (2004) have considered the sharp interface modeling approach by using semi-analytical models to find out how thick the Nile Delta aquifer's freshwater layer is.

Most of these earlier studies were hypothetical in nature because of a lack of salinity records for the NDA (Mabrouk et al. 2013; Sherif and Al-Rashed 2001). The NDA has been exposed to extensive groundwater pumping during the previous 30 years, suggesting that there is a significant dispersion zone between the intrusion of seawater inland into the NDA and freshwater (Mabrouk et al. 2013). The existence of a large dispersion zone was revealed according to field investigations and experiences (Sherif and Al-Rashed 2001). As a result, the variable density modeling approach is suitable for simulating the dynamic interactions between freshwater and saline water in the NDA (Mabrouk et al. 2013). Several researchers have presented different investigations into seawater intrusion into the NDA based on the dispersion zone modeling approach (Sherif et al. 1988, 1990; Darwish 1994; Amer and Sherif 1996; Sherif and Singh 1997; Sherif 1999; Sherif and Al-Rashed 2001; Sherif et al. 2012; Sefelnasr and Sherif 2014; Abdelaty et al. 2014; Abd-Elhamid et al. 2016; Abd-Elhamid et al. 2016).

Sherif and Al-Rashed (2001) utilized 2D-FED to simulate sweater intrusion in the NDA in the vertical direction. The ND model was utilized to determine the groundwater flow and the transition zone between seawater and freshwater. The saltwater line advanced further inland into the NDA to a distance approximately 63 kilometers from the sea shoreline. In addition, the freshwater line encroaches more into the NDA to a distance about 108 kilometers from the sea shoreline. A flux found with a minimum depth about 22 km, from the fresh groundwater to the saline water. RIGW (2002) presented the salinity concentrations contour maps in the NDA between 1960 and 2000. The maps led RIGW to the conclusion that development activities had an impact on salinity of groundwater in the NDA. Between 1980 and 1990, groundwater salinity rose, the freshwater line advanced

further inland in to the NDA indicating greater saline water intrusion.

Sherif et al. (2012) utilized FEFLOW to examine the seawater intrusion in the NDA in the horizontal direction. In 2D-dimensional actual vertical simulation, the notion of equal freshwater head was investigated. The simulation in the horizontal direction was carried out using four various horizontal sections at various levels (100, 200, 300, and 400 m), each with its own pressure head to determine the section depth. The results revealed that, with depth of 100 meters, a few kilometers of saltwater moved inland into the NDA. In addition, with depth of 200 meters, the dispersion zone advanced further inland in to the NDA to get to Tanta city. With depth of 300 meters, the saline water encroached more into the NDA to Mansoura city. Finally, with depth 400 meters, the seawater covers the whole active region of the domain.

Abdelaty et al. (2014) utilized SEAWAT code to examine the seawater intrusion in the NDA. In respect to RIGW, the data of TDS concentrations in several wells in 2008 was utilized. The outcomes of the NDA model revealed that the saltwater line advanced further inland in to the middle of the NDA, to a distance about 63.75 kilometers from the sea shoreline. In addition, the freshwater line encroached more into the middle of the NDA and get to 93.75 kilometers from the sea shoreline. Abd-Elhamid et al. (2016) utilized 2D-FEST code to simulate the groundwater flow and the salinity transport for studying the saline intrusion in the NDA considering the effects of climate change. The outcomes of the NDA model showed that the saltwater line moved more into the NDA to a distance of 64 kilometers from the sea shore line. In addition, the freshwater line advanced inland to reach to 112 kilometers at the middle cross section of the NDA.

Previous studies on seawater intrusion into the NDA have confirmed that seawater intruded inland by more than 100 km into the aquifer. Equi-lines of 35 and 1.0 g/l intruded inland into freshwater at the middle cross section of the NDA to a distance about 63 and 108 kilometers from the Mediterranean Sea's coastline (Sherif 1999; Sherif et al.2001, 2003; Abdelaty et al. 2014). Abd-Elhamid et al. (2016) demonstrated that concentration lines of 35000 and 1000 mg/l moved into the NDA to a distance about 61 and 110 km, respectively.

The IPCC predicts that, by 2100, global warming will cause a rise in sea levels of between 11 and 88 cm (IPCC 2001, 2007). Many researchers have predicted that a rise in sea level will origin substantial effects on groundwater resources in the coastal groundwater aquifers, as well as cause inland migration in the dispersion zone in between the freshwater and saline water (FAO 1997). The rise in Mediterranean Sea levels has had a substantial consequence on seawater intrusion into the NDA. The concentration line of 1,000 mg/l is expected to move inland into NDA to a distance about 9.0 km when the sea level rises to 1.0 m (Sherif 1999; Sherif and Al-Rashed 2001). A rise of 1.0 m will cause the saltwater line (35000 mg/l) to encroach inland into the NDA by about 10 km (Abd-Elhamid et al. 2016).

Nofal et al. (2015) utilized SEAWAT code to build a comprehensive GW model for the NDA considering the heterogeneity of the aquifer based on new observed data. The field data of GW level was used for calibration the model. The outcomes of simulation confirmed that fresh GW flow is not being lost to the sea from the NDA. The results introduced a good representation and visualization for interface between fresh and saline water as a foundation for future management of GW resources in the NDA. Mabrouk et al. (2018) assessed the situation of saline intrusion into the NDA utilizing SEAWAT code. Six different expected scenarios which combing the impact of increasing the groundwater abstraction and rise in sea level were tested. The outcomes of the tested scenarios confirmed that increasing the groundwater discharges has a significant effect on salinization process of freshwater in the NDA than the projected rise in Mediterranean sea level. The important findings of this study were determining the volume of freshwater, brackish and salinity water in the NDA system. The analysis of results can be used for adaptation and mitigation pans of seawater intrusion in the near future.

Abd-elhamid et al. (2019) investigated the potential effects of minimizing the Nile River flow as a result of GERD construction on saline intrusion in the NDA using SEAWAT code. Two expected filling scenarios of GERD was considered. The outcomes of the model confirmed the freshwater and saltwater lines advanced to distances of 110.2 and 70.85 km in case of filling the GERD reservoir in 3 and 6 years consequentially. In addition maintaining the freshwater system in the NDA required minimizing the groundwater discharge by 60 and 40% consequentially. Mabrouk et al. (2019.a) used SEAWAT code to evaluate the existing situation and introduce coming management and adaptation of saline intrusion in the NDA. The NDA model was tested for different management scenarios included groundwater discharge and expected rise in sea level. Three adapted scenarios were presented variation of crop pattern, artificial groundwater recharge through wells, and abstraction of brackish groundwater and reused after desalination practices.

Mabrouk et al. (2019.b) identified the critical zones for sweater intrusion in the NDA through building 3D model. The model outcomes confirmed the presence of groundwater salinization as a result of seawater intrusion in the NDA. The eastern and southwestern regions in the NDA showed increase in the TDS concentration as a result of increasing groundwater discharges and dissolution practices of marine limestone. Also, according to the findings, the NDA is still far from being in a condition of dynamic equilibrium. The groundwater modeling tool may be utilized to simulate coming saline intrusion situations in order to develop a long-term groundwater resource adaptation strategy. Abd-Elaty et al. (2021) mentioned that increasing the pumping discharges and projected rise in sea level causes advancement of seawater into the NDA.

Abd-Elaty et al. (2021) utilized SEAWAT code for simulating saline intrusion into the NDA taking into account future scenarios of pumping discharge and rise in sea level to find optimum GW well system for managing seawater intrusion. The outcomes confirmed that seawater intrusion can be retreaded by 19.5%, 6.2%, and 5.9% for the cases increasing GW recharge, minimizing groundwater

discharges, and brackish water abstraction. Agoubi (2021) explored the position of saline intrusion inland in to North Africa coastal area and presented a comprehensive literature for the extent of seawater intrusion in the area and the expected challenges in the future. The results showed that the seawater intrusion changes from country to other based on the groundwater discharges rate, hydrological conditions, urbanization development, economic management, and impacts of climate change. In addition a limitation is found to manage saline intrusion in the coastal aquifer of North Africa.

The NDA is from the coastal aquifers that are considered vulnerable to Mediterranean Sea saline intrusion. According to (Kashef 1983) the main sources of groundwater recharge for the NDA is from seepage from the Nile River, the irrigation canal networks and excessive irrigation water. The effects of groundwater recharge from the Nile Delta's irrigation canal systems on seawater intrusion can be observed in the upper clay layer nearby the Nile River and its tributaries (Sherif et al. 2012). Seawater advances towards the Nile Delta aquifer are accompanied by a decline in the water levels of irrigation canals (Abdelaty et al. 2014). In contrast, earlier research considered the groundwater recharge in groundwater modeling from ten canals, regardless of the fact that the ND region have intensive irrigation canal network. The main aim of this study is to use the SEAWAT program to simulate seawater intrusion into the NDA under various scenarios of climate change in relation to the actual irrigation canal networks in the ND area.

II. STUDY AREA DESCRIPTION

The NDA is regarded as one of the world's greatest underground reservoirs (Sherif and Al-Rashed 2001).The ND region is approximately 25000 km2, and located in the north of Egypt, (Sherif et al. 2012). The Mediterranean Sea bounds the ND region in the north, in the south, it is bordered by the Nile River, and it is bordered on the east by the Suez and Ismailia Canals, and on the west by the El-Nubaria Canal (Sherif et al. 2012). The Nile River is split into nine main canals in the ND region. The Rosetta and Damietta Branches are its two primary branches. The west branch, the Rosetta Branch, is roughly 239 kilometers long, while the east branch, the Damietta Branch, is around 245 kilometers long, as displayed in Fig. 1 (Kashef 1983).

The ND aquifer's groundwater system is regarded to be a complicated system. The Quaternary aquifer of the ND is a semi-confined. It is topped with a clay layer that ranges in thickness from the south to the north at the top of the earth's surface (Farid 1980; Wilson et al. 1979). The thickness of the NDA starts at 200 meters in the south and rises to 1,000 meters in the north (RIGW,1992). In the south, the overlying clay layer is 5 to 20 meters thick, whereas in the middle of the Nile Delta, it can reach 50 meters thick (Said 1962; Diab et al. 1997). In the winters of 2000 and 2010, groundwater recharge into the NDA varied between 0.0 mm in the south (Cairo) and 134 mm in the north (Alexandria), correspondingly. Percolation into the ND Quaternary aquifer occurs at a rate of 0.8 millimeters per day on average (DRI 1989). The rate of percolation is affected by the soil type as well as the irrigation and drainage systems in place (Warner et al. 1991), and varies from 0.25 to 0.8 millimeters/day in the central and southern parts and from 1.0 to 1.5 millimeters/day in the western desert. The minimum observed percolation rate is from 0.1 to 0.5 millimeters/day where both drip and sprinkler irrigation are commonly used (RIGW/IWACO 1990a).

III. METHODOLOGY

Hydraulic parameters

Many geological, hydrochemical, and hydrological specialists have investigated the NDA extensively in order to determine its properties. The vertically and horizontally hydraulic conductivity values of the clay cap, as assessed by several researches, are shown in Table A1. Previous investigations have estimated the hydraulic features of the ND Quaternary aquifer, as shown in Table A2. Farid (1980) published several hydraulic conductivity and the storage coefficient values for the NDA .The value of hydraulic conductivity in the NDA rises towards the west and south. The effective porosity of the NDA medium is thought to be around 0.3.The storage coefficient value has been estimated by the RIGW (1980) to be 2.5×10^{-3}. The transmissivity value varies between 15,000 and 75,000 m^2/day, according to RIGW (1990). The values of the longitudinal and the transverse dispersivity in the NDA were calculated to be 100 and 10 m, correspondingly, by Sherif et al. (1988), whereas the diffusion coefficient (D*) was estimated to be 10^{-4} m^2/day. From north to south, the distance between the ground surface and the groundwater table grows. It fluctuates between 1 and 2 meters in the north, grows to 3 to 4 meters in the central, and reached a maximum of 5 metres in the south (RIGW 2002; Morsy 2009). In Egypt, the RIGW managed an evaluation of the Nile Delta region's abstraction wells in 1992, 1995, 1997, 2002, and 2008. In 2008, the entire withdrawal from the ND aquifer's groundwater system was $3.48x10^6$ m^3/year (Abdelaty et al. 2014).

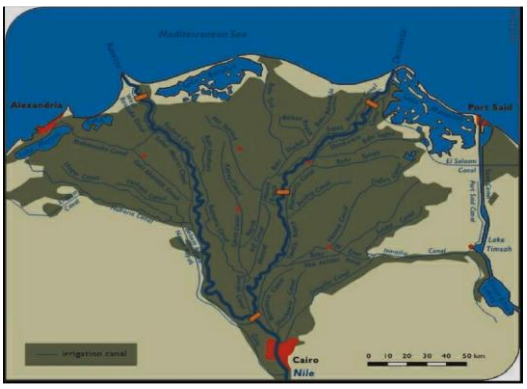

Fig. 1. Study area location and digitized map of irrigation canal networks in the Nile Delta region, Abd-Elhamid et al. (2016)

Numerical model

In this work, the SEAWAT code (Guo and Langevin 2002) is utilized for simulating seawater intrusion. This program solves coupled groundwater flow and the solute transport equations by combining MODFLOW and MT3DMS codes.

Variable density flow estimates are also performed using SEAWAT. The well-known Visual MODFLOW-2000 (version 4.6.0.168) utilized in the SEAWAT (version 4) program's variable density flow (VDF) process to solve the variable density equations using the finite difference approach (Guo and Langevin 2002). The current research used MT3DMS to solve solute transport formulations that are linked to the integrated MT3DMS transport process. While the VDF procedure in the SEAWAT program (Guo and Langevin 2002) calculated the variable density groundwater flow equation relating to the equivalent freshwater head. The IMT process in SEAWAT program solves the solute transport equation (Langevin et al. 2008).

Model geometry and boundary conditions

For the initial conditions, and according the data limitations, the author has considered the initial conditions as explained by previous studies. The concentration at the western boundary is constant and equal to that of freshwater. A hydrostatic pressure distribution in the vertical direction is considered for the freshwater flux via the land side boundaries. The aquifer's bottom is impermeable. The aquifer is replenished with freshwater from the irrigation network at the top border, which is a leaky boundary, and the concentration is equivalent to that of freshwater (The gradient of concentration is zero). For the Mediterranean Sea boundary, the concentration is equal to seawater concentration. The flux across this boundary is inwardly directed. At this point, the pressure is hydrostatic, while at sea level, it is atmospheric. According to the initial conditions described above, the SEAWAT program is utilized for simulating the groundwater flow and saline intrusion into the NDA. There are 292 columns and 190 rows in the NDA model domain, with a resolution of 1.0 km, as shown in Fig. 2.

The domain depth varied from 1,000 m in the north at the Mediterranean Sea's coastline and decreased towards the south to reach 200 m. Three vertical cross sections in the western, central, and eastern regions of the ND are displayed in Figures 3.a, b, and c. The constructed domain is split into 11 levels, with the clay layer at the top, while the subsequent layers from two to 11 signify the Quaternary aquifer. The upper clay layer thickness increases from 25 m in the south direction towards the north direction to reach 50 m. Based on the literature and the field measurements by the RIGW, the southern head boundary is defined as a constant head equal to 16.96 m Above Mean Sea Level (AMSL (Abdelaty et al. 2014).

A zero value on the Mediterranean Sea coastline defines the upper head border in the north. The eastern boundary condition in the right is defined as free flowing when considering Suez Canal recharge. The Ismailia Canal runs through the southeast corner of the domain, with the recorded field's water level beginning at 16.17 m AMSL in the south and ending at 7.01 AMSL in the east. The Rayah El-Behery and El-Nubaria Canals divide the southwestern domain, with the recorded field's water level ranging from 16.00 m AMSL in the south to 0.50 m AMSL in the north (Abdelaty et al. 2014). Earlier research (Abdelaty et al. 2014) provided data for 2008 on the water level of the Nile Delta's principal canals and drains; see Table A3 in the Appendix.

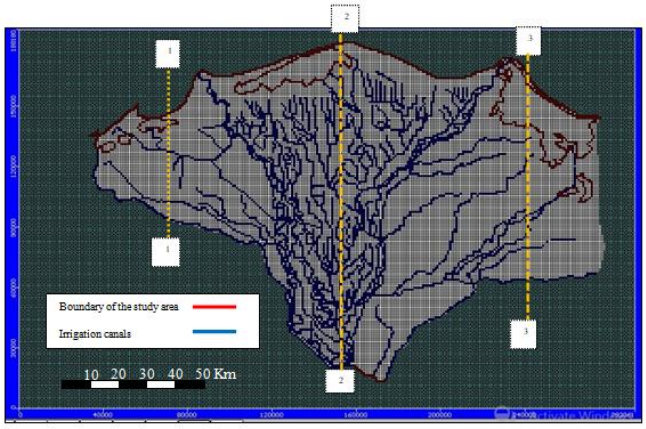

Fig. 2. Model geometry and discretization

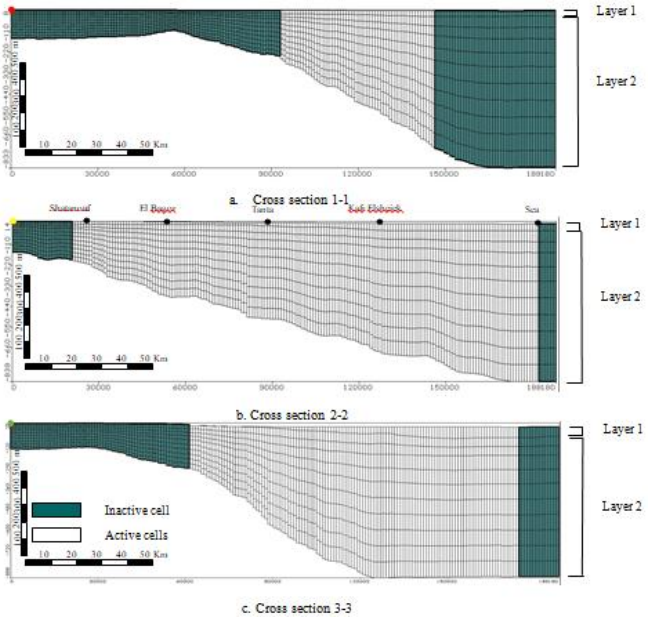

Fig. 3. Vertical crosses sections in the Nile Delta aquifer model: a) 1-1, b) 2-2 and c) 3-3

The bank level of irrigation canals and their upper width were previously calculated by Armanuos et al. (2016) and consequently utilized in constructing the NDA model (see Table A4 in the Appendix). The Nile Delta's main and branch canals have typical water depths of 2.0 and 3.0 meters, respectively (Dahab 1993).The river package interface in the MODFLOW software was utilized in order to include the Rosetta and Damietta Branches, the rayahs and the main canals in the built ND model. The river MODFLOW package required the hydraulic properties of the input canals, which includes the water level, the bottom level, and the hydraulic conductivity of the river bed, river bed thickness and conductance of the riverbed. The seepage from the surface system into the groundwater depends on the conductance value of the river, the streams and the general head boundary conditions, which can be calculated using the following mathematical expression.

$$C = \frac{LxWxK}{M} \quad \text{.....(1)}$$

Where: C is the riverbed conductance [L^2/T], L is the river's reach length in each grid cell. [L], W is the width of each grid cell's riverbed [L], K is the river bed hydraulic conductivity [L/T] and M is the thickness of the riverbed in each grid cell [L].

Table. A5 in Appendix presents the hydraulic conductive of selected canals in the current study compared with previous studies. The hydraulic conductance (m^2/day) for the current model exceeds the value assigned by Morsy (2009) for the representative canals. The location map showing the distribution of production and observation wells in the NDA, established on data collected by the RIGW in 2008, is shown in Fig. A1 in the Appendix. The total volume of abstraction from the NDA equaled $2.78x10^9$ m^3/year in 2008 (Abdelaty et al. 2014). As showed in Fig. A1, the concentration was set at 40000 mg/l in the northern boundary (the Mediterranean Sea coastline) and 35000 mg/l in the eastern boundary (the Suez Canal coastal line) (Abdelaty et al. 2014). The initial state of the groundwater concentration was set at 0 mg/l (Abdelaty et al. 2014).

Studied scenarios

According to the IPCC, ocean levels will rise between 0.11 and 0.88 meters by 2100 as a result of global warming (IPCC 2001, 2007). In the first scenario, the SEAWAT code was utilized for simulating the impact of sea level rises by 25, 50, 75 and 100 cm on seawater intrusion into the NDA in 2025, 2050, 2075 and 2100, respectively. In the last 30 years, the total annual groundwater pumping from the NDA has grown substantially. Egypt's RIGW recorded a rise from $1.6x10^9$ m^3/year in 1980 to $3.5x10^9$ m^3/year in 2003, eventually reaching $4.6x10^9$ m^3/year in 2010, (Mabrouk et al. 2013).The yearly abstraction rate is projected to reach $0.20x10^9$ m^3 per year (Mabrouk et al. 2013). In the second scenario: the SEAWAT code was utilized for predicting the seawater intrusion into the NDA under extra groundwater abstraction conditions, where the maximum decline in the groundwater table is observed near the southern boundary are 25, 50, 75 and 100 cm in 2025, 2050, 2075 and 2100, respectively. In scenario 3: based on the first and second situations combined, the SEAWAT code was utilized to investigate seawater intrusion into the NDA.

Model calibration and validation

The NDA model was run numerous times throughout the calibration procedure to reduce the difference between the simulated head and the measured head by the RIGW in 2008 (see Fig. A2). For each parameter, sixty dispersed observation wells were selected from the research region and calibrated up to the maximum discrepancy between the observed and simulated groundwater head level was 0.60 m. (see Fig. A3).For NDA model validation, the measured groundwater head levels were compared with the simulated results for the extra 60 records (see Fig. A4). So as to validate the model for saltwater intrusion, the length of the seawater wedge in the NDA at three different cross sections was compared to that reported in previous studies.

Fig. A5a displays the calibrated values of the vertical hydraulic conductivity kv of the first clay layer, which varies from 0.01 to 0.025 m/day. Fig. A5b displays the calibrated value of the horizontal hydraulic conductivity kh of the second layer, which varies from 50 to 240 m/day. Fig. 4 shows the simulated groundwater levels in the NDA. Fig. 5a introduced a comparison between the measured and simulated groundwater levels for 60 GW well records, prepared by the RIGW in 2008, following a calibration process (see Fig. A6 in the Appendix) involving different observation wells (Morsy 2009). The R2 and RMSE with reference to the measured and simulated groundwater levels were 0.98 and 0.75m, correspondingly. Table A6 displays the calibrated values of the NDA model parameter.

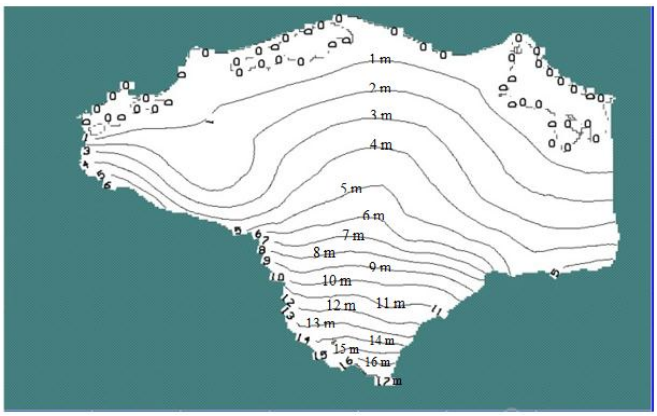

Fig. 4 Simulated groundwater head in the Nile Delta aquifer in 2008

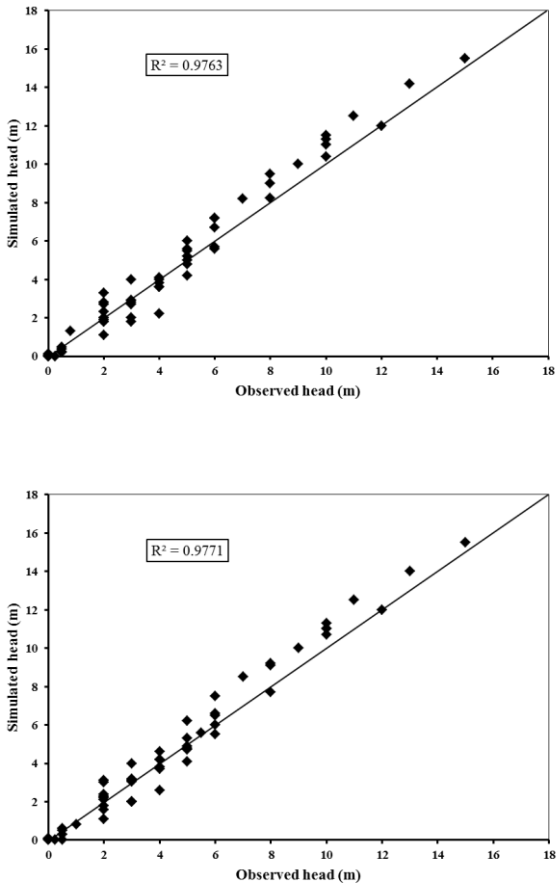

Fig. 5. Relationship between observed and simulated groundwater levels for 60records for (a) Calibration process and (b) Validation process

A comparison of measured and predicted groundwater levels for another 60 recordings chosen for NDA model validation is shown in Fig. 5b. The correlation coefficient R2 was 0.9771, and the RMSE was 0.70 m. The SEAWAT code was utilized to recognize the transition zone in the NDA, which was relied on a variable density modeling approach.

The TDS variations in the NDA were visualized using horizontal and vertical cross sections. Sec 1-1, Sec 2-2, and Sec 3-3 are three cross sections in the vertical direction were found, with depth variations extending from the south (land side) to the north (sea side) (coastline). Cross sections (1-1), (2-2), and (3-3) were placed to the west, center, and east parts of the ND, correspondingly, as previously indicated and depicted in Fig. 4-c. As a result, the depths of these cross sections were 240, 200, and 200 m in the south and 900 m in the north. Cross sections (1-1), (2-2), and (3-3) were 70, 150, and 120 kilometers long, respectively, as displayed in Fig. 4a-c. The current model's validation procedure started with the year 2008. Fig. 6 presents the distributions of TDS in the NDA in the horizontal view for the base case.

Concerning the base case, for the three nominated cross sections: (1-1), (2-2) and (3-3), the transition zone is located within TDS concentrations of 35000 mg/l (saltwater line) and 1000 mg/l (freshwater line). The width of this transition zone is the distance between these two lines. For cross section (1-1), in the current model, the transition zone width is 26 km and the results show that the saltwater and freshwater lines encroach inland to a distance approximately 40.0 km and 66 km, correspondingly (see Fig. 7a). Fig .7b shows the simulation results for the current model for cross section (2-2). From this figure, compared with Fig. 7a, the saltwater and freshwater lines intrude more than for cross section (1-1), with values of 56 and 105 km, respectively. The transition zone width of this section is 49 km. In cross section (3-3), the saltwater line encroaches inland to a distance approximately 74.0 km, while the freshwater line encroaches to a distance approximately 100.0 km, where the transition zone width equals 26.0 km, as shown in Fig. 7c.

Regarding the calibration and validation process for saltwater distribution, Table 1 compares the saltwater wedge's length in the NDA in the current model and previous findings. The observed salinity concentrations were compared using simulated values for model calibration and validation (Morsy 2009; see Fig. A7).

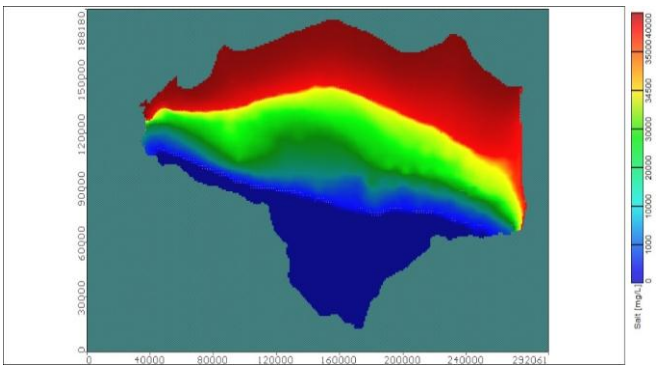

Fig. 6. Horizontal distribution of TDS in the Nile Delta aquifer for the base case (year2008)

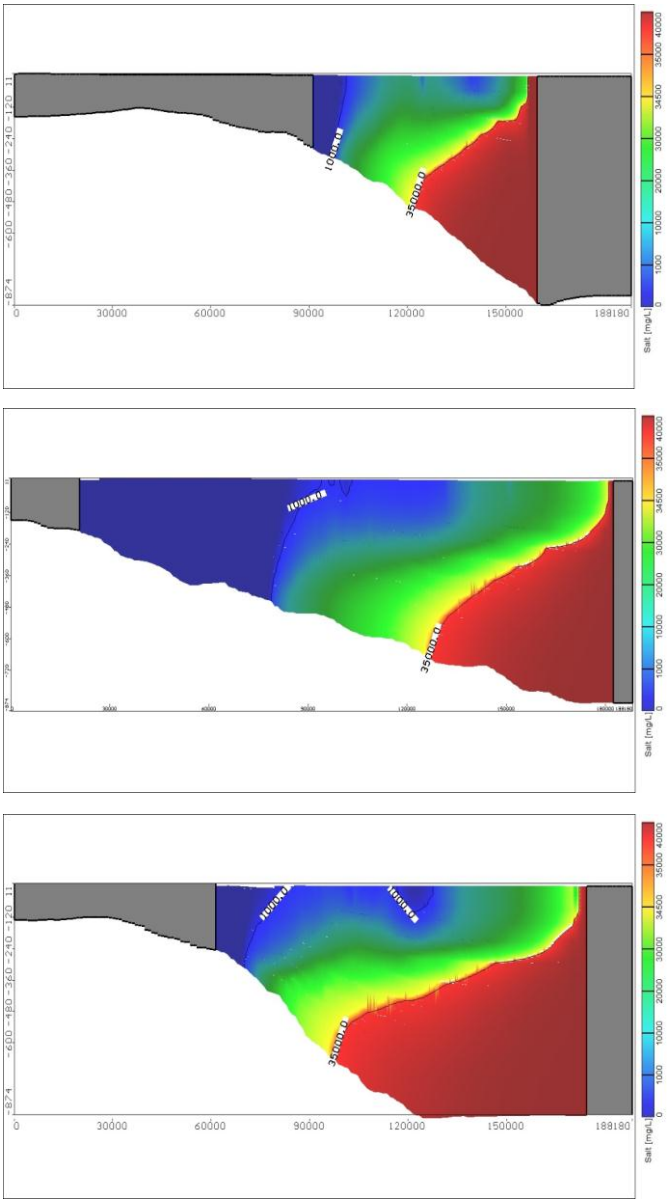

Fig. 7. Vertical Distribution of TDS in the Nile Delta aquifer at Sec 1-1, Sec 2-2 and Sec 3-3 at the base case (2008)

Fifty records of salinity concentration by the RIGW for 2008 were selected and compared with the salinity concentration for the model calibration, while another 50 records were selected for a model validation comparison (see Fig. A8 and Fig. A9 respectively). The results are acceptable in respect of the length of the intruded saltwater at the three different cross sections (see Table 1), as shown in Figs. 9 and 10.

The results of the current SEAWAT model, with its comparison of previous model results (2D-FEST, 2D-FED and SEAWAT, as shown in Table.1) show good agreement in the TDS distribution at the three cross sections, as reported by Abd-Elaty et al. (2014). Fig. 8a compares the observed and simulated concentration for 50 records, which were selected for NDA model calibration. The R^2 equals

0.9881 and the RMSE equals 1,802 mg/l. Fig. 8b compares the observed and simulated salinity concentration for the other 50 records, which were selected for NDA model validation. The R2 with regard to the observed and simulated values equals 0.9886 and the RMSE equals 2,404 mg/l. When the real irrigation canal networks are included in the current NDA model, seawater intrudes inland into the aquifer over a substantially shorter distance than Abd-Elaty et al. 2014 estimated in the base scenario at the similar cross sections. As per earlier studies, which did not consider the real irrigation canal networks in simulating the seawater intrusion into the NDA, the resultant groundwater recharge was fewer than the real one involved in the present NDA model.

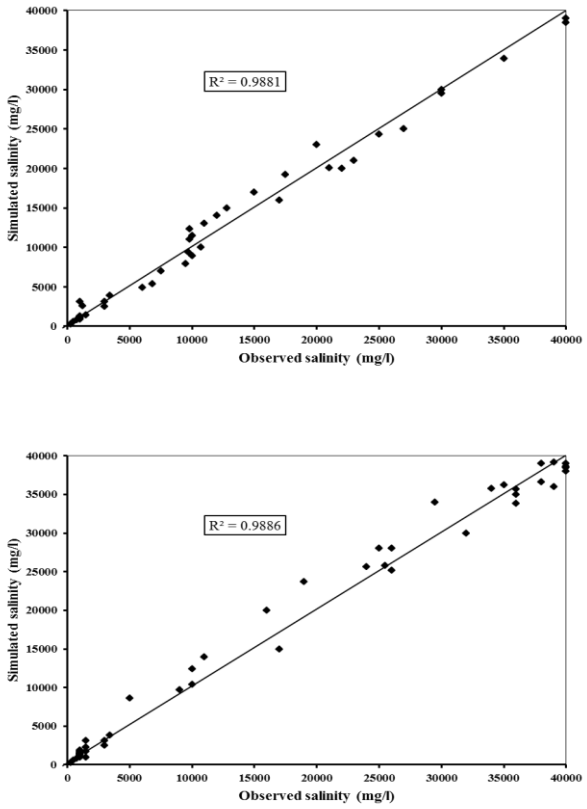

Fig. 8. Relationship between observed and simulated salinity concentration for 50records for (a) Calibration process and (b) Validation process

IV. Results and Discussion

After model validation, the present model was utilized for predicting the degree of the seawater intrusion into the NDA for 2025, 2050, 2075 and 2100 for the three supposed conditions: rise in sea level; rate changes in pumping out groundwater; and a combination of both conditions.

A. Scenario 1: Impact of sea level rise on the extent of seawater intrusion into the NDA

The present model was utilized for simulating the impact of rise in sea level on saltwater intrusion into the NDA by 25, 50, 75 and 100 cm in 2025, 2050, 2075 and 2100, respectively. According to this timescale, for Cross Section (1-1), rise in sea level intrude the saltwater line at distances of 44.19, 44.51, 44.63 and 44.65 km, respectively, while the freshwater line consequently intrudes by 67.90, 68.00, 68.57 and 68.84 km from the shoreline, as shown in Fig. 9.

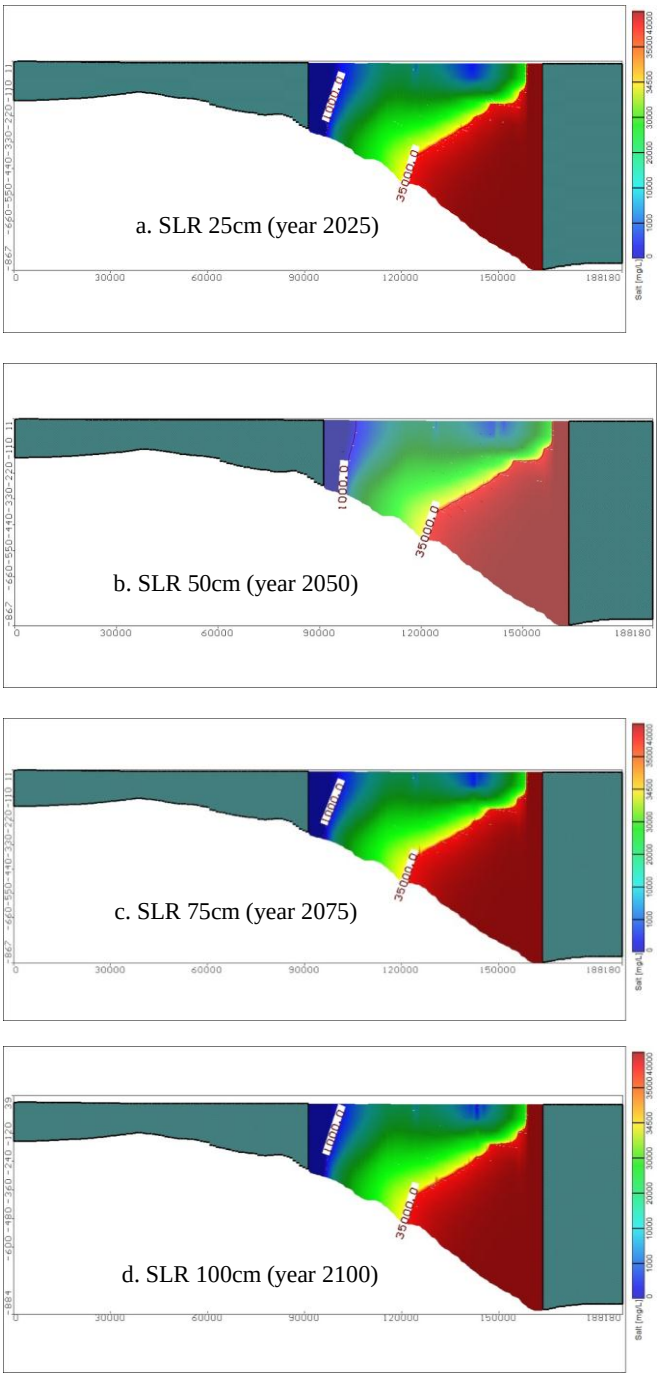

Fig. 9. Vertical Distribution of TDS in the Nile Delta aquifer at Sec 1 at SLR 25, 50, 75 and 100 cm

For Cross Section (2-2), rise in sea level of 25, 50, 75 and 100 cm cause the saltwater line to encroach into the NDA at distances about 58.35, 59.05, 59.75 and 60.25 km, respectively, while the freshwater line consequently moves toward the inland to distances of 106.9, 107.4, 107.5 and 108.2 km, as measured from the sea shoreline, as presented in Fig. 10.

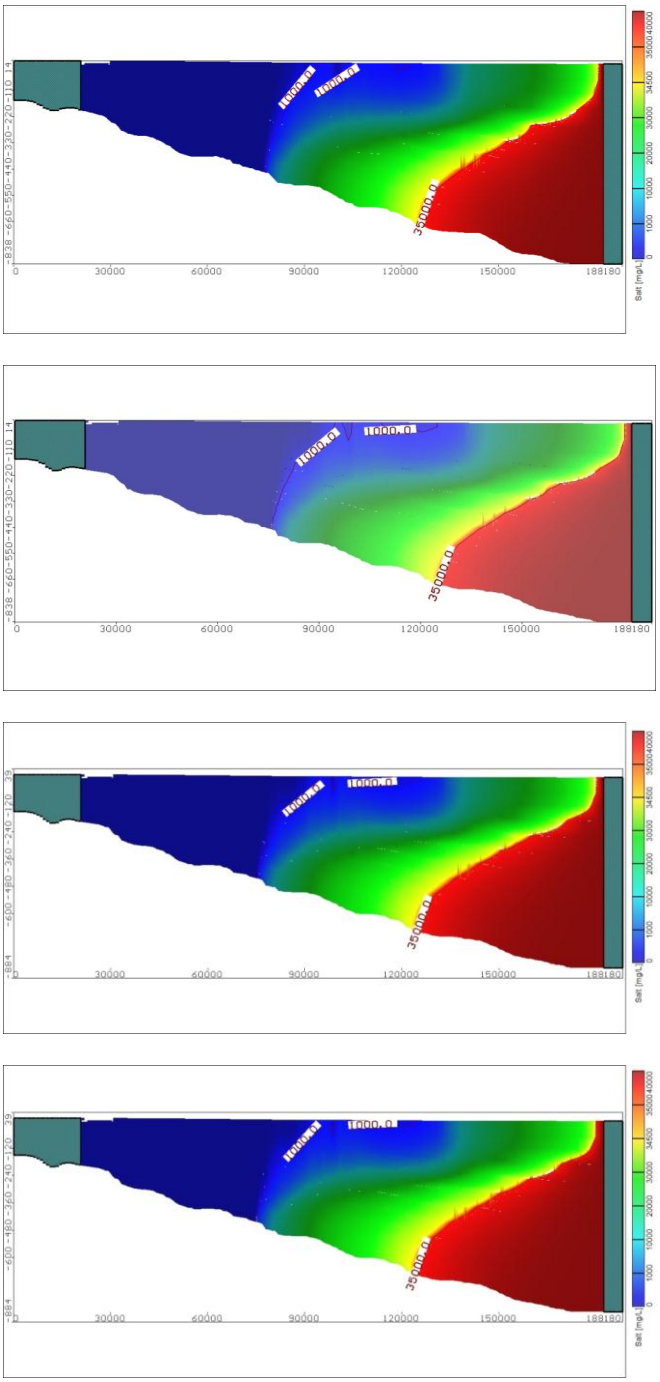

Fig. 10 Vertical Distribution of TDS in the Nile delta aquifer at Sec 2 at SLR 25, 50, 75 and 100 cm

In Cross section (3-3), a rise in the sea level of 25, 50, 75 and 100 cm causes the saltwater line to encroach into the NDA to distances about 79.11, 81.10, 81.62 and 82.20 km, respectively, while the freshwater line consequently intrudes to distances of 105.5, 105.6, 106.3 and 106.5 km from the shoreline, as shown in Fig. 11. The rise in seawater levels in the Mediterranean Sea has imposed additional heads of saline water on the sea side, such that saltwater has advanced further into the NDA. In comparison with the base case, the seawater line has advanced more inland to distances of 5.11, 7.10, 7.62 and 8.2 km with a sea level rise of 25, 50, 75 and 100 cm, respectively, while the freshwater line has advanced more at distances of 5.5, 5.6, 6.3 and 6.5 km, respectively, in comparison with the current base case.

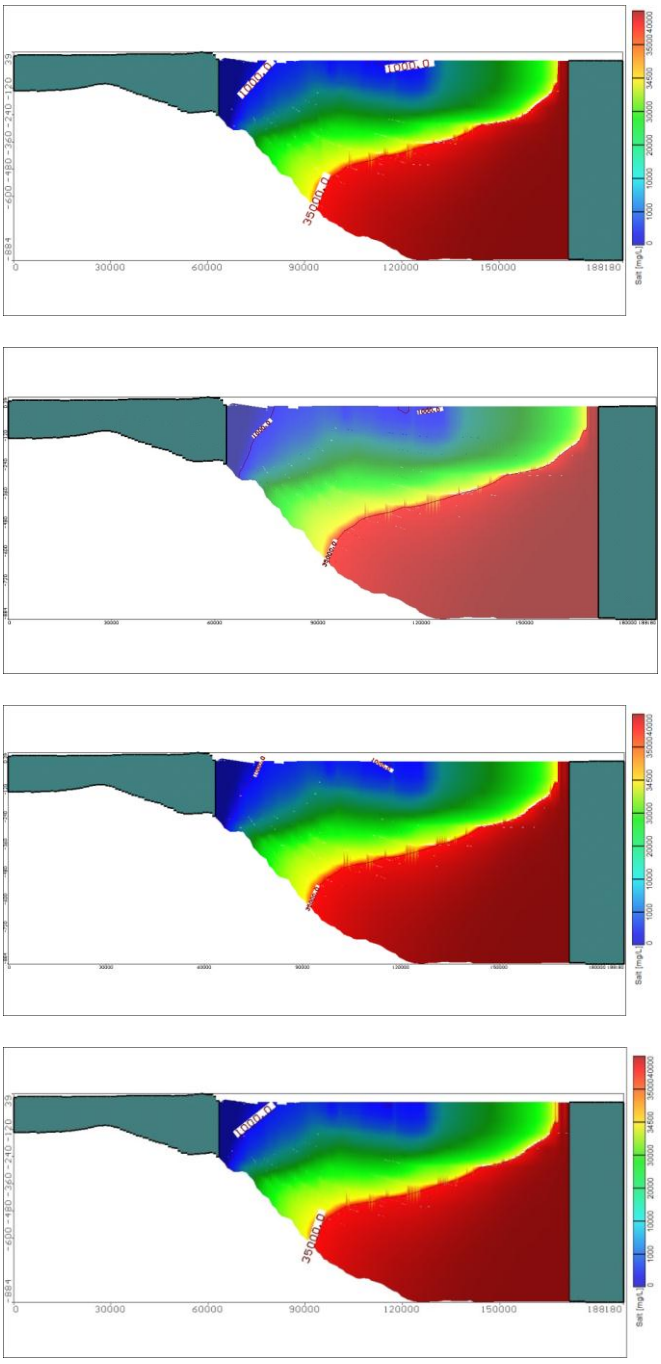

Fig. 11 Vertical Distribution of TDS in the Nile delta aquifer at Sec 3 at SLR 25, 50, 75 and 100 cm

B. Scenario 2: Rate change in pumping out groundwater on the extent of seawater intrusion in the NDA

Under increased groundwater pumping conditions, the model was utilized to estimate seawater intrusion into the NDA, on the basis that the lower boundary's groundwater head declines by 25, 50, 75 and 100 cm in 2025, 2050, 2075 and 2100, respectively. In Cross Section (1-1), to the west, a decline in the lower boundary's groundwater head by 25, 50, 75 and 100 cm forces the ND aquifer's saltwater line to encroach to a distances approximately 44.03, 44.09, 44.15

and 44.27 km, respectively, while the freshwater line consequently intrudes at distances of 67.82, 67.84, 67.88 and 68.02 km from the sea shoreline, as presented in Fig. 12.

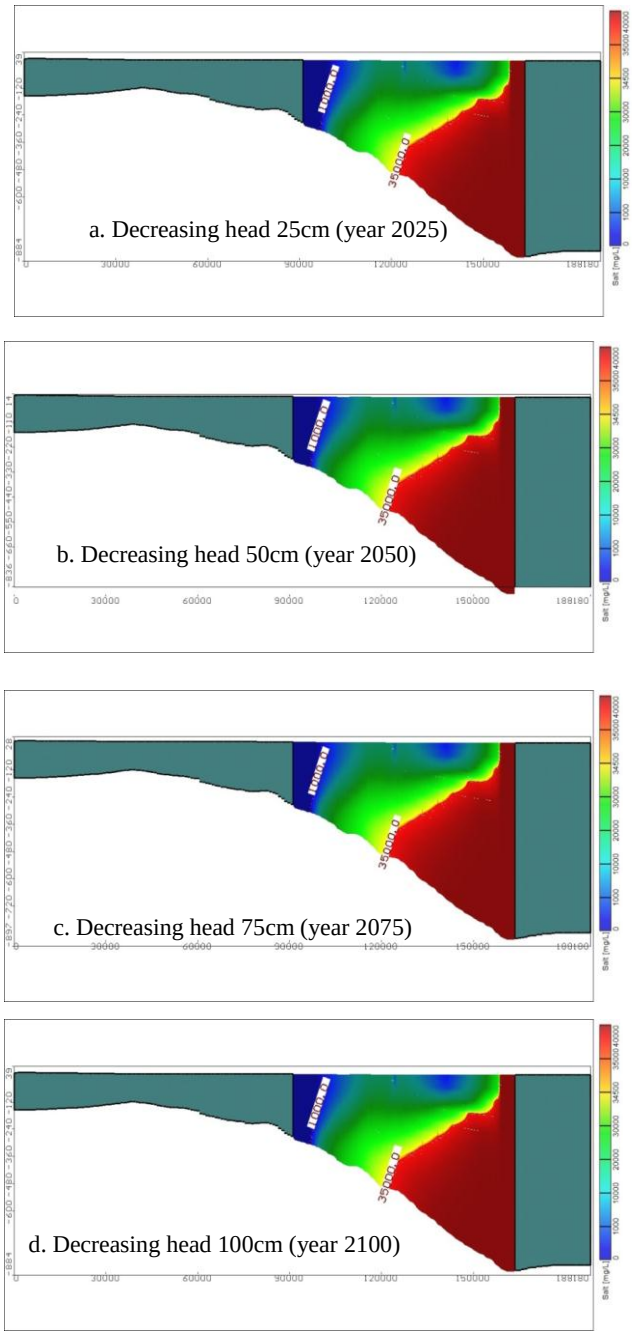

Fig. 12 Vertical distribution of TDS in the Nile Delta aquifer at Sec 1 at decreasing head by 25, 50, 75 and 100 cm

For Cross section (2-2), a decline in the lower boundary's groundwater head by 25, 50, 75 and 100 cm and the seawater line encroaches into the NDA at distances around 58.19, 58.25, 58.45 and 58.47 km, respectively, while the freshwater line consequently advances into the NDA at distances around 106.1, 106.2, 106.3 and 106.4 km from the sea shoreline, as displayed in Fig. 13.

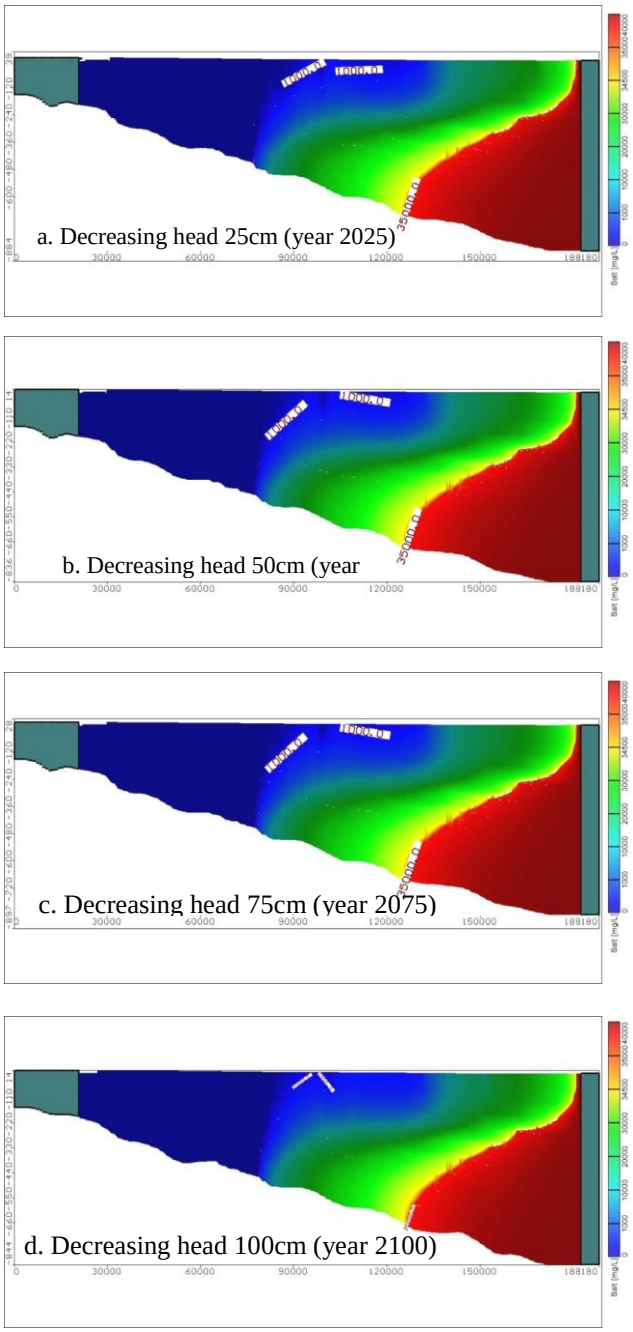

Fig. 13 Vertical distribution of TDS in the Nile Delta aquifer at Sec 2 at decreasing head by 25, 50, 75 and 100 cm

In Cross section (3-3), to the east, a decline in the lower boundary's groundwater head by 25, 50, 75 and 100 cm leads the seawater line to encroach at distances approximately 79.30, 79.47, 79.52 and 79.75 km, respectively, while the freshwater line consequently intrudes at distances of 105.2, 105.3, 105.5 and 105.5 km from the sea shoreline, as displayed in Fig. 14. A decline in the lower boundary's groundwater head, as a result of further groundwater abstraction, causes a decline in the velocity and flow of freshwater from the south towards the north, causing the saltwater to intrude further towards the freshwater into the NDA.

The seawater line moves further into the NDA to additional distances approximately 5.30, 5.47, 5.52 and 5.75 km, along with a decline in the lower boundary's groundwater head, as a result of further groundwater abstraction, by 25, 50, 75 and 100 cm, respectively, in comparison to the default situation. On the other hand, the freshwater line advances more into the NDA by additional distances approximately 5.2, 5.3, 5.4 and 5.5 km, respectively, in comparison with the current base case.

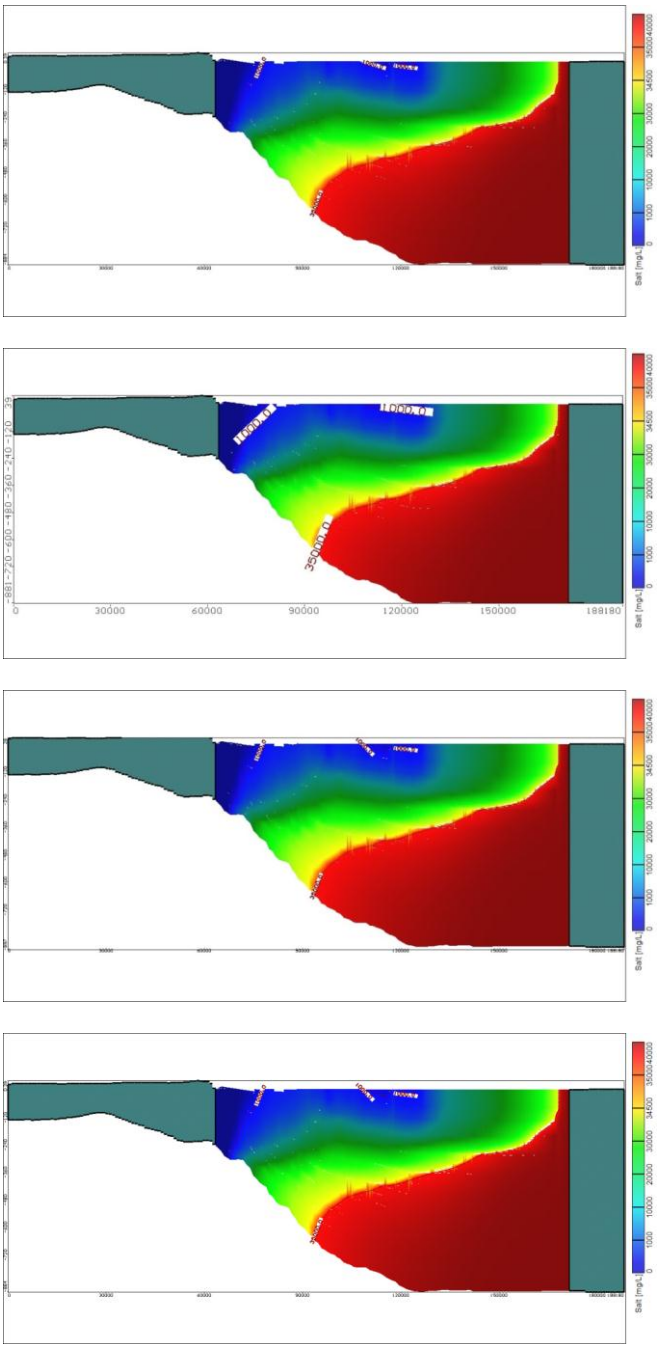

Fig. 14. Vertical distribution of TDS in the Nile Delta aquifer at Sec 3 at decreasing head by 25, 50, 75 and 100 cm

C. Scenario 3: Combination of the Scenario 1 and Scenario 2 conditions

With the combined impact of the first and second scenarios, the present model was implemented to explore seawater intrusion into the NDA, on the following bases: rise in sea level by 25 cm and a 25-cm decline in groundwater head in 2025; rise in sea level by 50 cm and a 50-cm decline in groundwater head in 2050; rise in sea level by 75 cm and a 50-cm decline in groundwater head in 2075; rise in sea level by 100 cm and a 100-cm decline in groundwater head in 2100. In Cross section (1-1), rise in sea level and a groundwater head decline of 25, 50, 75 and 100 cm results in advancement of the seawater line into the NDA to distances approximately 44.28, 44.50, 44.55 and 44.64 km, respectively, while the freshwater line consequently intrudes by 67.80, 68.00, 68.53 and 69.00 km from the sea shoreline, as displayed in Fig. 15.

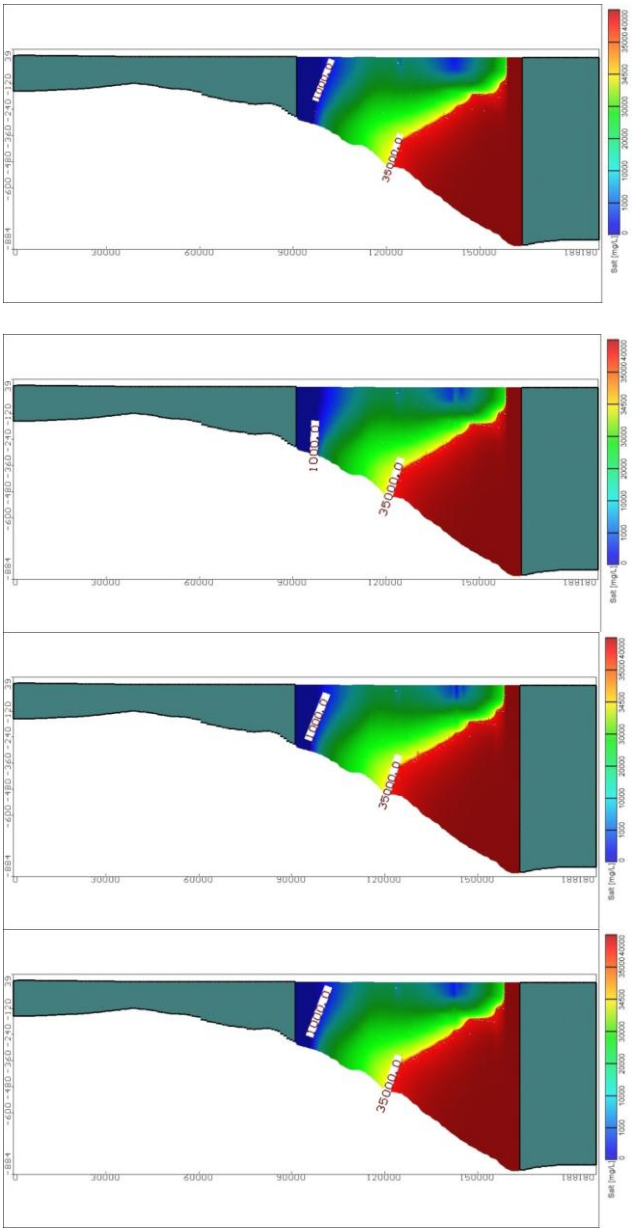

Fig. 15. Vertical distribution of TDS in the Nile delta aquifer at Sec 1 at SLR and decreasing head by 25, 50, 75 and 100 cm

For Cross section (2-2), rise in sea level and a decline of lower boundary's groundwater head of 25, 50, 75 and 100 cm encroach the seawater line more into the NDA at distances approximately 59.00, 59.43, 59.96 and 60.50 km, respectively, while the freshwater line consequently advances inland to distances of 107.2, 107.3, 107.6 and 109.8 km from the sea shoreline, as displayed in Fig. 16.

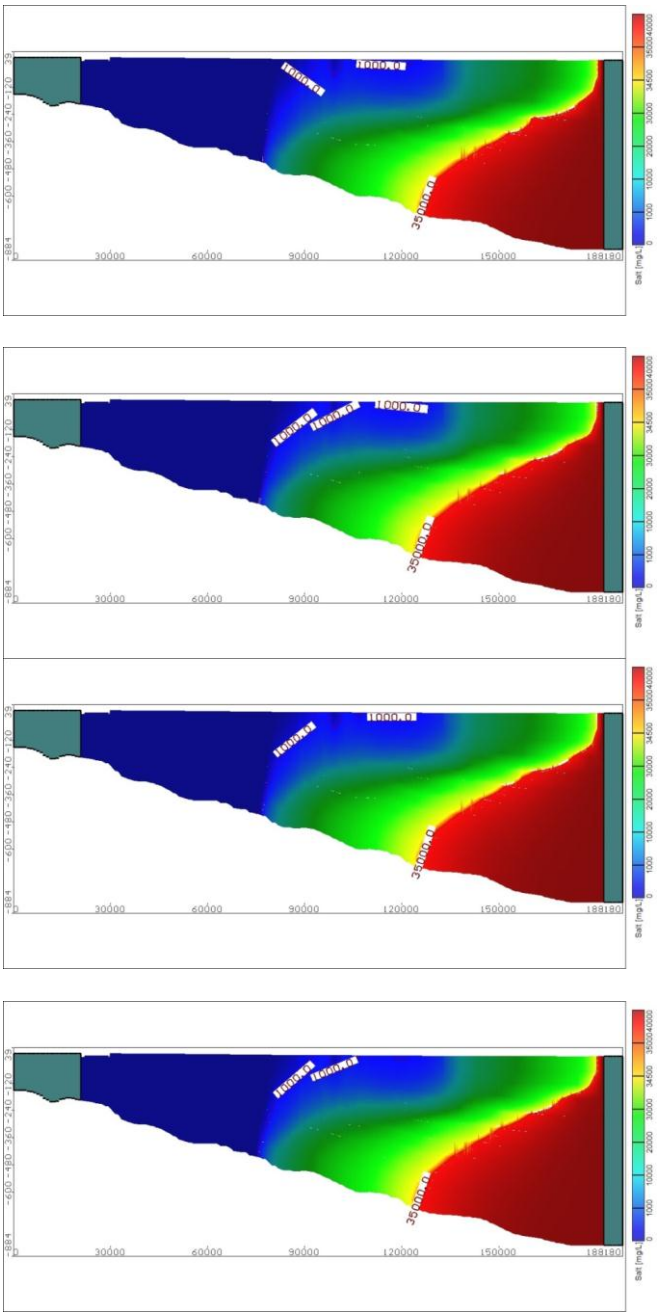

Fig. 16 Vertical distribution of TDS in the Nile delta aquifer at Sec 2 at SLR and decreasing head by 25, 50, 75 and 100 cm

In Cross section (3-3), to the east, the combination of rise in sea level and a decline of lower boundary's groundwater head of 25, 50, 75 and 100 cm cause the seawater line to move more into the NDA at distances approximately 81.22, 81.73, 82.20 and 84.20 km, respectively, while the freshwater line consequently intrudes at distances of 105.6, 106.4, 106.7 and 107.0 km from the sea shoreline, as displayed in Fig. 17. The saltwater advances further inland into the NDA in scenario 3 as the combination of rise in sea level and a decline of lower boundary's groundwater head, as a result of further groundwater abstraction results in a further decline in the freshwater flow and velocity, in addition to an additional head of seawater on the sea side. The saltwater line encroaches more inland into the NDA at distances approximately 7.22, 7.73, 8.20 and 10.20 km, along rise in sea level of 25, 50, 75 and 100 cm and a decline of lower boundary's groundwater head, as a result of further groundwater abstraction of 25, 50, 75 and 100 cm, respectively. Meanwhile, the freshwater line advances additional into the NDA at distances around 5.5, 6.4, 6.7 and 7.0 km, respectively, in comparison with the current base case.

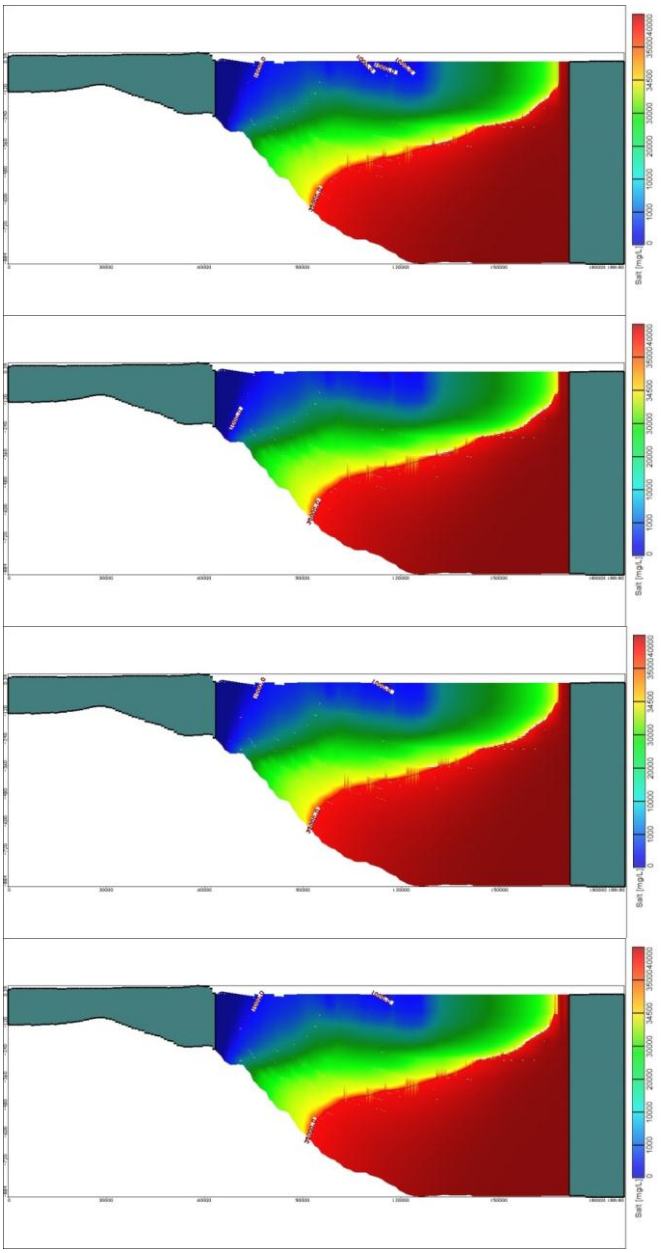

Fig. 17 Vertical distribution of TDS in the Nile Delta aquifer at Sec 3 at SLR and decreasing head by 25, 50, 75 and 100 cm

D. Comparative study

Table 2 compares the intrusion length of the saltwater line in the central cross section of the NDA in the current model and the results obtained by Abd-Elaty et al. (2014). The comparison shows that saltwater intrudes into the NDA at small distances compared with those reported by Abd-Elaty et al. (2014) in the base case, and for various scenarios of sea level rise and a decline of lower boundary's groundwater head, as a result of further groundwater abstraction.

In comparison with the results for TDS distribution presented by Abd-Elhamid et al. (2016) using the 2D-FEST program, the results of the present NDA model confirmed that the saltwater and freshwater lines advance more into the NDA (as compared to the base case) at a smaller distance than reported by Abd-Elhamid et al. (2016). The saltwater and freshwater lines advance more inland into the NDA at distances approximately 8.2 and 6.5 km with sea level rise of 100 cm, in comparison to 9.0 and 10.0 km, respectively, as reported by Abd-Elhamid et al. 2016. Declining the lower boundary's groundwater head, as a result of further groundwater abstraction, causes the saltwater and freshwater lines to advance into the NDA at distances of 5.75 and 5.5 km, compared with 6.0 and 8.0 km, respectively, as reported by Abd-Elhamid et al. (2016). The saltwater and freshwater lines advance further into the NDA at distances around 10.2 and 7.0 km with a rise in sea level of 100 cm and a decline in the lower boundary's groundwater head as a result of further groundwater abstraction, compared with 14.0 and 15.0 km, respectively, as reported by Abd-Elhamid et al. (2016).

Using the SEAWAT code to include the real irrigation canal networks in the present model of the NDA, seawater encroaches inland into the NDA at shorter distances than those described by Sherif et al. (2001, 2003), Abd-Elaty et al. (2014), and Abd-Elhamid et al (2016) Due to various climate change scenarios, including sea level rise and a decline of lower boundary's groundwater head, at similar cross sections. Because all earlier researches utilized various codes (2D-FED, 2D-FEST, and SEAWAT) for predicting the degree of seawater intrusion into the NDA without taking into account the real irrigation canal networks, the resulting groundwater recharge could be lower than the one presented in the current model.

V. CONCLUSION

An integrated three-dimensional groundwater model for the NDA was built by the SEAWAT program, and included groundwater recharge from all irrigation canals, which has not been considered in previous simulation studies on saltwater intrusion into the NDA under various conditions. Three proposed scenarios were tested: rise in sea level; decreases in the southern head boundary as a result of further groundwater abstraction; and a combined impact of both the first and the second proposed scenarios. The results show that, after considering the real irrigation canal networks in the existing model, saltwater intrudes inland into the NDA at relatively smaller distances than those reported in earlier researches at the similar cross sections under the proposed various scenarios. A proposed rise in sea level of 25, 50, 75 and 100 cm causes the saltwater line to advance inland at distances of 5.11, 7.10, 7.62 and 8.2 km, respectively, in comparison with the current base case. Moreover, in comparison to the base situation, a decline in the lower boundary's groundwater head as a result of additional groundwater abstraction of 25, 50, 75 and 100 cm in the southern boundary intrudes the saltwater line further inland at distances of 5.30, 5.47, 5.52 and 5.75 km, respectively. The impact of decreases in the groundwater head at the southern boundary on seawater intrusion into the ND is much less than the impacts of rise in sea level. The dispersion zone between the saltwater and freshwater advances further inland into the aquifer when combining sea level rises and decreases in the lower boundary's groundwater head because of extra groundwater abstraction. The worst presented case is scenario 3, in which saltwater intrudes further inland than in the first and second scenarios, where the saltwater line advances further inland into the aquifer at distances of 7.22, 7.73, 8.20 and 10.20 km, respectively, in comparison with the base situation. The present model's findings could be used decision makers and authorities to identify locations most vulnerable to seawater intrusion into the NDA, as well as to manage groundwater resources in the ND region. Future strategies are therefore essential for the adaptation and mitigation of saltwater intrusion into the NDA.

REFERENCES

Abd-Elhamid H, Javadi A, Abdelaty I, Sherif M (2016) Simulation of seawater intrusion in the Nile Delta aquifer under the conditions of climate change, Hydrology Research, 47(5), 1-14, DOI: 10.2166/nh.2016.157.

Wilson J, Townley LR, and Sa Da Costa A (1979) Mathematical development and verification of a finite element aquifer flow model AQUIFEM-1, Technology Adaptation Program, Report No. 79–2, M.I.T., Cambridge, Massachusetts.

Amer A, Farid MS (1981) About sea water intrusion phenomenon in the Nile Delta aquifer. In Proceedings of the International Workshop on Management of the Nile Delta Groundwater Aquifer. CU/Mit, Cairo.

Farid MS (1980) An approach to handle sea water intrusion in the Nile Delta aquifer, RIGW, Faculty of Engineering, Cairo University, Egypt.

Farid MS(1985) Management of groundwater system in the Nile Delta, Ph.D. thesis, Faculty of Engineering, Cairo University, Egypt.

Sakr SA, Attia FA, Millette JA (2004) Vulnerability of the Nile Delta aquifer of Egypt to seawater intrusion, International conference on water resources of arid and semi-arid regions 25 of Africa, Issues and challenges, Gaborone, Botswana.

Mabrouk MB, Jonoski A, Solomatine D, Uhlenbrook S (2013) A review of seawater intrusion in the Nile Delta groundwater system – the basis for assessing impacts due to climate changes and water resources development, Hydrol. Earth Syst. Sci. Discuss., 10, 10873–10911, doi: 10.5194/hessd-10-10873-2013, 2013.

Sherif MM, Al-Rashed MF (2001) Vertical and Horizontal Simulation of Seawater Intrusion in the Nile Delta Aquifer, First International Conference on Saltwater Intrusion and Coastal Aquifersó Monitoring, Modeling, and Management. Essaouira, Morocco, April 23ñ25, 2001.

Sherif MM, Singh VP, Amer AM (1988) A two-dimensional finite element model for dispersion (2D-FED) in coastal aquifer, J. Hydrol., 103,11–36, doi: 10.1016/0022-1694(88)90003-0.

Sherif MM, Singh VP, and Amer AM (1990) A note on saltwater intrusion in coastal aquifers, J. Water Resour. Manage., 4, 113–123.

Darwish MM (1994) Effect of probable hydrological changes on the Nile Delta aquifer system, Ph.D. thesis, Cairo University, 1994.

Amer A, Sherif MM (1996) An integrated study for seawater intrusion in the Nile Delta aquifer. Working Paper for SRP, NWRC-MPWWR, Cairo, Egypt.

Sherif MM, Singh VP (1997) Groundwater Development and Sustainability in the Nile Delta Aquifer. Final Report, Binational Fulbright Commission, Egypt.

Sherif MM (1999) The Nile Delta aquifer in Egypt, Chapter 17 in Seawater Intrusion in Coastal Aquifers, concepts methods and practices, edited by: J. Bear, A. Cheng, S. Sorek, D. Ouazar, and A. Herrera, Theory and Application of transport in porous media, Kluwer academic publishers, the Netherlands, 14, 559–590.

Sherif MM, Sefelnasr A, Javadi A (2012) Incorporating the concept of equivalent freshwater head in successive horizontal simulations of seawater intrusion in the Nile Delta aquifer, Egypt", Journal of Hydrology, 186–198, pp. 464–465, DOI:org/10.1016/ j.jhydrol.2012.07.007.

Sefelnasr A, Sherif M (2014) Impacts of seawater rise on seawater intrusion in the Nile Delta aquifer, Egypt. Groundwater, vol. 52, no. 2, pp. 264–276.

Abdelaty IM, Abd-El hamid HF, Fahmy MR, Abdelaal GM (2014) Investigation of some potential parameters and its impacts on saltwater intrusion in Nile Delta aquifer, Journal of Engineering Sciences, Assiut University, Faculty of Engineering, 42:(4), 931-955.

Abd-Elhamid HF (2016) Investigation and control of seawater intrusion in the Eastern Nile Delta aquifer considering climate change, Water Science & Technology: Water Supply, 16(5), 1-13, DOI: 10.2166/ws.2016.129.

RIGW (2002) Nile Delta groundwater modeling report, Research Inst. For Groundwater, Kanater El-Khairia, Egypt.

Sherif M. M., Al-Rashed M. F., Vertical and Horizontal Simulation of Seawater Intrusion in the Nile Delta Aquifer, First International Conference on Saltwater Intrusion and Coastal Aquifersó Monitoring, Modeling, and Management. Essaouira, Morocco, April 23ñ25, (2001).

Intergovernmental Panel of Climate Change (IPCC). 2001. Climate change 2001: Impacts, adaptations, and vulnerability. Contribution of Working Group II to the third assessment report of the Intergovernmental Panel on Climate Change. Cambridge, UK, and New York: Cambridge University Press.

Intergovernmental Panel of Climate Change (IPCC). 2007. Climate change 2007: Impacts, adaptations, and vulnerability. Contribution of Working Group II to the fourth assessment report of the Intergovernmental Panel on Climate Change. Cambridge, UK: Cambridge University Press.

Nofal ER, M.A. Amer, S.M. El-Didy & Akram M. Fekry (2015) Delineation and modeling of seawater intrusion into the Nile Delta Aquifer: A new perspective, Water Science, 29:2, 156-166, DOI: 10.1016/j.wsj.2015.11.003

Mabrouk, M.; Jonoski, A.; H. P. Oude Essink, G.; Uhlenbrook, S. Impacts of Sea Level Rise and Groundwater Extraction Scenarios on Fresh Groundwater Resources in the Nile Delta Governorates, Egypt. Water 2018, 10, 1690. https://doi.org/10.3390/w10111690

Abd-Elhamid, H., Abdelaty, I. & Sherif, M. Evaluation of potential impact of Grand Ethiopian Renaissance Dam on Seawater Intrusion in the Nile Delta Aquifer. Int. J. Environ. Sci. Technol. 16, 2321–2332 (2019). https://doi.org/10.1007/s13762-018-1851-3

Mabrouk, M.; Jonoski, A.; Oude Essink, G.H.P.; Uhlenbrook, S. Assessing the Fresh–Saline Groundwater Distribution in the Nile Delta Aquifer Using a 3D Variable-Density Groundwater Flow Model. Water 2019, 11, 1946. https://doi.org/10.3390/w11091946

Mabrouk, M., Jonoski, A., & Essink, G.O. (2019). REGIONAL GROUNDWATER MODELLING FOR DETERMINING ADAPTATION STRATEGIES IN THE NILE DELTA AQUIFER.

Abd-Elaty, I., Javadi, A.A. & Abd-Elhamid, H. Management of saltwater intrusion in coastal aquifers using different wells systems: a case study of the Nile Delta aquifer in Egypt. Hydrogeol J (2021). https://doi.org/10.1007/s10040-021-02344-w

Agoubi, B. A review: saltwater intrusion in North Africa's coastal areas—current state and future challenges. Environ Sci Pollut Res 28, 17029–17043 (2021). https://doi.org/10.1007/s11356-021-12741-z

Abd-Elhamid HF, (2010) A Simulation-Optimization Model to Study the Control of Seawater Intrusion in Coastal Aquifers .PhD Thesis, University of Exeter, UK.

Kashef (1983) Salt-water intrusion in the Nile Delta, Groundwater, 21, No. 2, doi: 10.1111/j.1745-6584.1983.tb00713.x.

RIGW (1992) Hydrogeological map of Nile Delta. Scale 1: 500,000. 1st Edn. ND. 1992a.

Said R (1962) The geology of Egypt, Amsterdam, the Netherlands: Elsevier.

Diab, M. S., Dahab, K., and El Fakharany, M.: Impacts of the paleohydrological conditions on the groundwater quality in the northern part of Nile Delta, The geological society of Egypt, J. Geol., 4112B, Cairo, 779–795, 1997.

DRI Drainage Research Institute, Cairo, Egypt, (1989) Land Drainage in Egypt, edited by: Amer, M. 5 H. and de Ridder, N. A., Drainage Research Institute, Cairo, Egypt.

Warner JW, Gates TG, Attia FA, Mankarious WF (1991) Vertical leakage in Egypt's Nile Valley: Estimation and implications, J. Irrig. Drain Eng.-ASCE, 117, 515–533, doi: 10.1061/(ASCE)0733-9437(1991)117:4(515).

RIGW/IWACO (1990) hydrological inventory and groundwater development plan western Nile Delta region, TN77. 01300-9-02 Research Inst. for Groundwater, Kanater El-Khairia, Egypt, 1990a.

Morsy WS (2009) Environmental management to groundwater resources for Nile Delta region, PhD thesis, Faculty of Engineering, Cairo University, Egypt.

Guo, W. and Langevin, C. D.: User's Guide to SEAWAT: A Computer Program for Simulation of Three-Dimensional Variable-Density Groundwater Flow, Techniques of Water-Resources Investigations Book 6, Chapter 7, 77 pp., (2002).

Langevin CD, Daniel T, Thorne J, Alyssa M, Dausman MC, Weixing G (2008) SEAWAT Version 4: A Computer Program for Simulation of Multi-Species Solute and Heat Transport. Techniques and Methods Book 6, Chapter A22. U. S. Department of the Interior, U.S. Geological Survey.

Armanuos AM, Negm A, Yoshimura C, Valeriano OCS (2016) Estimatiom of bed and bank levels of an irrigation canal network towards accurate groundwater modeling of the Nile Delta aquifer, International Water Technology Journal, 6(1),pp.74-84.

Dahab KA (1993) Hydrological evaluation of the Nile Delta after the High dam construction, thesis of Ph.D, Faculty of science, Monofia University, Egypt, 30.

Table 1. Comparison between saltwater wedge length in the Nile Delta aquifer for the current model and previous studies

	(Sherif 1999; Sherif et al. 2001, 2003)		Abd-Elhamid (2016)		Abd-Elhamid et al. (2016)		Abd-Elaty et al. (2014)		Current model	
Sec.	2D-FED		SEAWAT		2D-FEST		SEAWAT		SEAWAT	
	Equi-line 35 (km)	Equi-line 1 (km)	Equi-line 35 (km)	Equi-line 1 (km)	Equi-line 35 (km)	Equi-line 1 (km)	Equi-line 35 (km)	Equi-line 1 (km)	Equi-line 35 (km)	Equi-line 1 (km)
West	-----	----	-----	-----	42.00	68.00	41.0	69.00	40.00	66.00
Middle	63.00	108.0	----	-----	64.00	112.0	61.0	110.0	56.00	105.00
East	-----	----	75.75	90.25	58.00	109.0	56.00	108.0	74.00	100.00

Table 2. Comparison between the intruded length of the saltwater line of current study and Abd-elaty et al. (2014) for different scenarios of climate change at section II (in the middle)

Case	Scenario	Current study	(Abd-elaty et al. 2014)
		Intrusion length (Km)	Intrusion length (Km)
Base case	Current situation	56.00	61.00
SLR	25	58.35	66.75
	50	59.05	67.00
	75	59.75	-------
	100	60.25	67.75
Increasing pumping discharges	25%	58.19	66.50
	50%	58.25	66.50
	75%	58.45	-----
	100%	58.47	65.75

Appendix

Table A1. The hydraulic properties of the top clay layer in the Nile Delta

Study	K_h(m/day)	K_v(m/day)
Farid (1980)	0.2160	0.0025
Farid (1985)	------	0.05
Anon (1980)	-----	0.0025
(RIGW/IWACO 1990a)	0.2505	0.0484
Wolf (1987)	0.1037	0.0011
(Sherif et al. 1988)	------	0.05
Warner et al. (1991)	0.2160	0.0073
RIGW (1992)	0.05-0.5	0.0025
Dahab (1993)	-----	0.01-10.0
Arlt (1995)	0.3800	0.0046
Sherif (2003)	--------	0.0025
Sakr and Mabrouk (2006)	10.0	0.15-16
El Arabei (2007)	0.1-0.25	0.01-.025
Fadlelmawla1and Dawoud (2006)	------	0.05-0.1
Sherif et al. (2012)	------	0.0005-0.005
Abdelaty et al. (2014)	0.1-0.25	0.01-.025
Nofal et al. (2015)	0.05-0.5	0.0025
Morsy and El-Fakharany (2012)	0.1- 0.25	0.01-0.025

Table A2. The hydraulic parameters of the Quaternary aquifer

Study	Horizontal Hydraulic Conductivity (K_x) (m/day)	T (m^2/day)	S Storage coefficient	Effective Porosity (%)
RIGW (1992)	35–100	15,000–75,000	10^{-4}-10^{-3}	-----
UNDP (1981)	55–103	20,000–103,000	10^{-4}-10^{-3}	---------

Anon (1980)	**100**	**-------**	**---------**	**------**
Farid (1980)	**112**	**72,000**	**$2.53x10^{-3}$**	**32-35**
Zaghloul (1985)	**119**	**-------**	**10^{-4}-10^{-3}**	**20–28**
Shahien (1987)	**50**	**2500–25,900**	**10^{-5}-10^{-4}**	**23–25**
Laeven (1991)	**150**	**10,350–59,800**	**----------**	**------**
Shahin (1991)	**35**	**------**	**-------**	**-------**
(RIGW/IWACO 1990a)	**35-75**	**25,000**	**----------**	**------**
Mabrook et al. (1983)	**72–108**	**----------**	**$0.72x10^{-4}$-$2.3x10^{-4}$**	**21–30**
Sollouma and Gomaa (1997)	**23–65**	**-----**	**---------**	**----**
Shata and El Fayoumy (1970)	**86**	**71,800**	**$1.1x10^{-3}$**	**----**
Bahr (1995)	**75**		**$1.1x10^{-3}$**	**18**
Dahab (1993)	**50-240**	**3,000-15,000**	**9.0×10^{-4}-1×10^{-1}**	**11.5-19**
RIGW/IWACO (1999)				
Southern ND	**50–100**	**5000–25, 000**	**-----**	**25–30**
Northern ND	**Less than 50**	**--------**	**--------**	**More than 30**
Sherif (1999)	**70-100**	**--------**	**---------**	**12-19**
Sherif and Al-Rashed (2001)	**100**	**--------**	**10^{-4}-10^{-3}**	**30**
Sherif (2003)	**100**	**----------**	**10^{-4}-10^{-3}**	**30**
El Arabei (2007)	**5-100**	**-------**	**5×10^{-4}-1×10^{-3}**	**20-60**
Tahlawi et al. (2008)	**35-75**	**500-25,000**	**------**	**------**
Sherif et al. (2012)	**36-240**	**2000-15000**	**-------**	**25-40**
Morsy and El-Fakharany (2012)	**20-55**	**--------**	**2.35×10^{-3}**	**25**
Abdelaty et al. (2014)	**5-100**	**--------**	**5×10^{-4}-1×10^{-3}**	**20-60**
Mazei et al. (2014)	**100-120**	**--------**	**---------**	**-------**
Elshinnawy et al. (2015)	**23.0-180.0**	**-------**	**--------**	**--------**

Table A3. Average water level of samples of canals in the Nile Delta in 2008 measured by RIGW

Name of canal	A.W.L
Mit Yazeid canal	**+5.80**
El Kassed canal	**+7.10**
Kotor canal	**+5.20**
El Ramadei canal	**+3.20**
El Moheit canal	**+3.30**
Nesheil canal	**+4.50**
Samoul canal	**+4.15**
Bahr Seif	**+6.85**
El Korashia canal	**+8.55**
El Bagoria canal	**+11.9**
El Kadei canal	**+5.90**
Shobra El Namla canal	**+7.85**
Damat canal	**+5.65**
Om Rabeih canal	**+6.30**
El Betanonia canal	**+7.65**
Semela canal	**+5.85**
Asei canal	**+6.65**
Heset Shabshir canal	**+6.15**
El Nehnaia canal	**+6.90**
Rossetta branch	**+12.96**
Damettia branch	**+13.38**
El Rayah El Tawfiky	**+13.96**
El Rayah El Menoufi	**+14.66**
El Nubaria canal	**+15.92**
Ismailia canal	**+15.68**
Bahr Elk Baqur Drain	**+12.35**
El Sharkawia canal	**+15.85**
El Basosia canal	**+15.93**
Bahr Moas canal	**+12.25**
Dorwa canal	**+16.25**
El Nagar canal	**+14.20**
El Nagaiel canal	**+15.80**
Kafr Bolein canal	**+7.900**
El Raiah El Naseri	**+16.21**
Seriakos regulator	**+14.60**
Gamgra regulator	**+10.15**
El Bagoria regulator	**+12.95**
El Nagar regulator	**+14.20**
El Karnein regulator	**+10.20**
Meleig regulator	**+10.20**

El Santa reguator	**+8.100**
El Kataba regulator	**+12.80**
El Basosia weir	**+15.62**
El Nehnaia lock	**+14.98**
Damietta Branch-Benha	**+10.80**
Damietta Branch -El Mansuora	**+2.18**
Damietta Branch- Sherbin	**+1.75**
Damietta Branch -Farskor	**+1.55**
Rosetta Branch-El Katatba	**+6.70**
Rosetta Branch- Abe El Hawei	**+3.80**
Rosetta Branch-Zawiat El Bahr	**+2.05**
Rosetta Branch-Kafr El Zaiat	**+2.05**
Rosetta Branch-Shobraeit	**+1.95**
Rosetta Branch-El Atf	**+1.94**
Rosetta Branch-Rashid	**+0.10**

Table A4. Upper canal width and bank level of samples of irrigation canals in the Nile Delta

Name of canals	Bank level (m) +MSL	Length of canal (km)	Upper canal width (m)
Bahr Shebin	**7.2,7.0**	**16.8**	**49**
Atf canal	**14.2,12.0**	**32.2**	**34.1**
El Halwanei canal	**5.0,1.0**	**19.50**	**12.4**
El Doon canal	**2.1,1.2**	**18.5**	**16.4**
Abou Halal canal	**3.8,2.2**	**8.6**	**9.5**
Mansour canal	**5.4,2.5**	**8.00**	**4.50**
EL Raiah El Twafiq	**20.5,2.0**	**160.0**	**49.0**
Wadei canal	**10.4,1.5**	**80.0**	**65.10**
Bahr Sageir	**8.5,1.3**	**65.0**	**35.0**
Boaheia canal	**12.8,6.0**	**50.0**	**21.50**
El Raiah El Beheriei	**19.0,12.5**	**80.00**	**87.0**
El Nobaria canal	**11,3.0**	**110.0**	**79.0**
East Kahnat canal	**8.6,5.0**	**44.0**	**38.0**
canal project Naser	**3.4,-2.0**	**11.50**	**19.00**
Hamed meneis canal	**4.5,-2.0**	**14.00**	**9.30**

Table A5.Hydraulic conductive of selected canals in the current study compared with previous studies

Canal Name	Hydraulic conductance	
	Morsy (2009)	The current study
Rossetta Branch	**500-800**	**600-1200**
Damietta Branch	**500-800**	**500-1100**
El Rayah El Tawfiky	**500-350**	**500-800**
El Rayah El Monoufi	**300-400**	**300-900**
El Nubaria Canal	**200-300**	**400-800**
Ismailia Canal	**200-300**	**400-800**

Table. A6 Calibrated values of Nile Delta aquifer model parameter

Hydraulic parameter	Layer No.	
	Clay layer (Layer 1)	Quaternary aquifer (Layer 2 to 11)
Horizontal hydraulic conductivity	**0.25 m/day**	**50 to 240 m/day**
Vertical hydraulic conductivity	**0.01 to 0.025 m/day**	**5.0 to 24.0 m/day**

List of Abbreviations

Abbreviations	Definition
ND	**Nile Delta**
NDA	**Nile Delta Aquifer**
IPCC	**Inter-governmental panel of climate change**
FAO	**Food and Agriculture Organization**
RIGW	**Research Institute of groundwater of Egypt**
GW	**Groundwater**
GERD	**Grand Ethiopian Renaissance Dam**
3D	**Three dimensional**
TDS	**Total dissolved solids**
DRI	**Drainage research Institute**
VDF	**Variable density flow**
AMSL	**Above mean sea level**

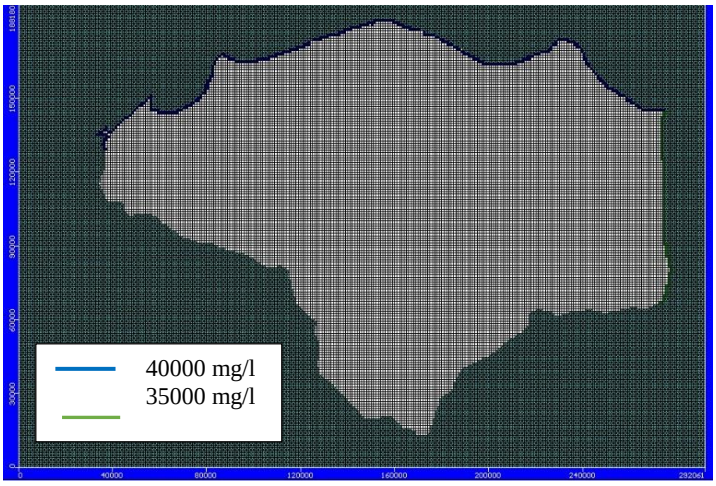

Fig. A1. Concentration boundaries in the Nile Delta model

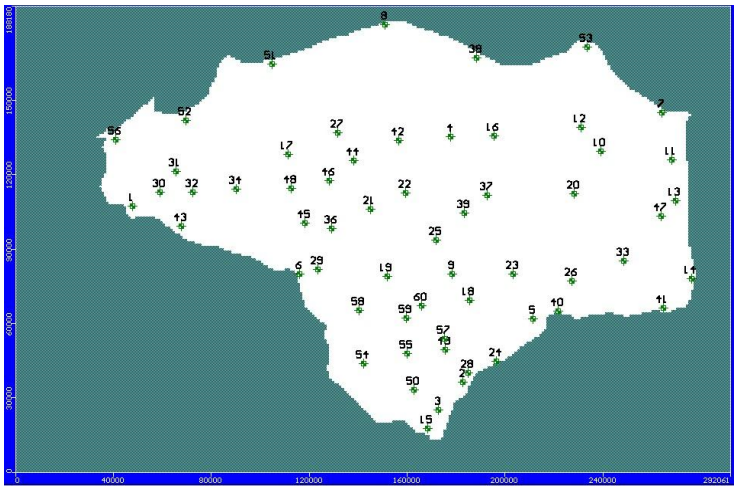

Fig. A2. Calibration points

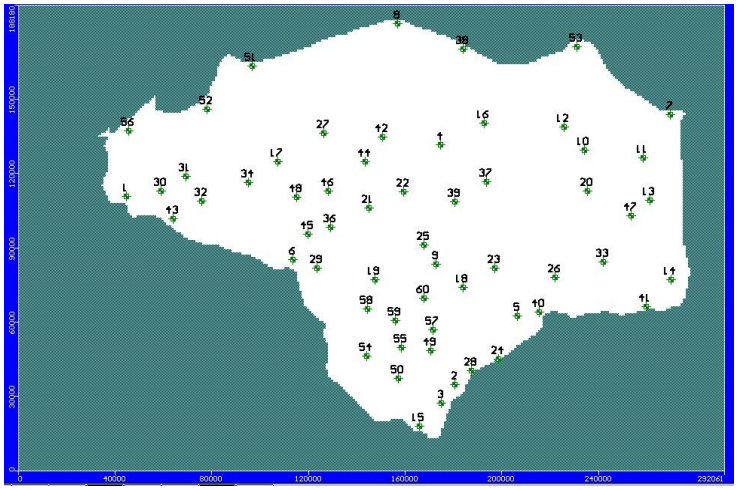

Fig. A3. Validation points

Fig. A4. Observed groundwater level in the Nile Delta aquifer (2008) (Morsy 2009)

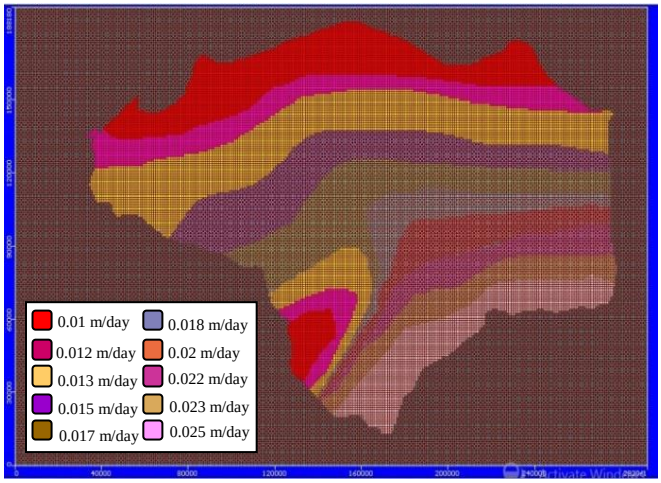

a Calibrated vertical hydraulic conductivity of the first layer

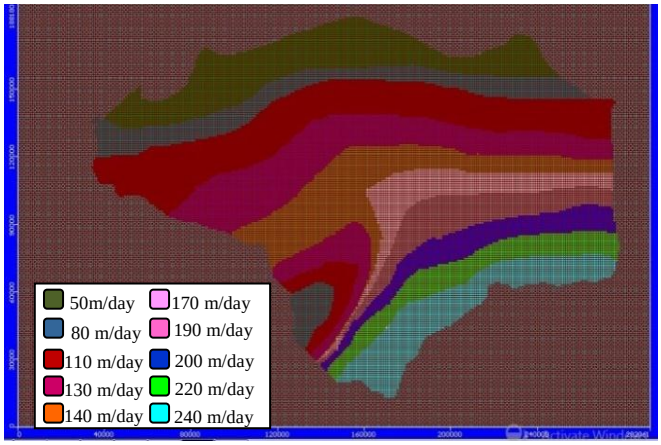

.b Calibrated horizontal hydraulic conductivity of the second layer

Fig. A5. Calibrated range of hydraulic conductivity of Nile Delta aquifer, Dahab (1993)

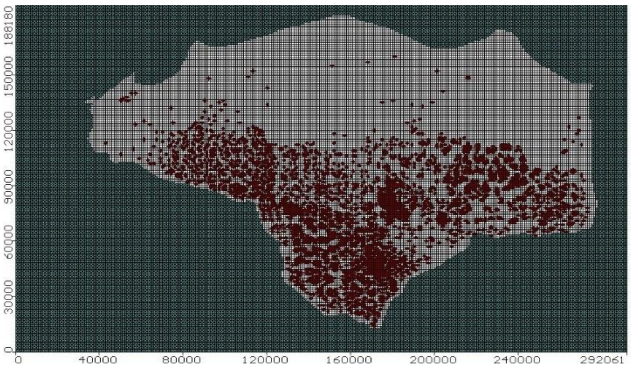

Fig. A6. Location map of extraction wells in the current model based on the collected data by RIGW (Abdelaty et al. 2014)

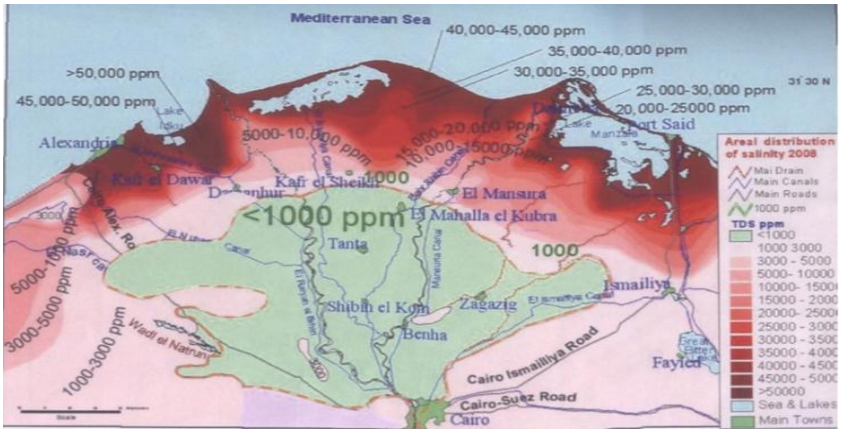

Fig. A7. Salinity distribution in the Nile Delta aquifer (2008), Morsy 2009

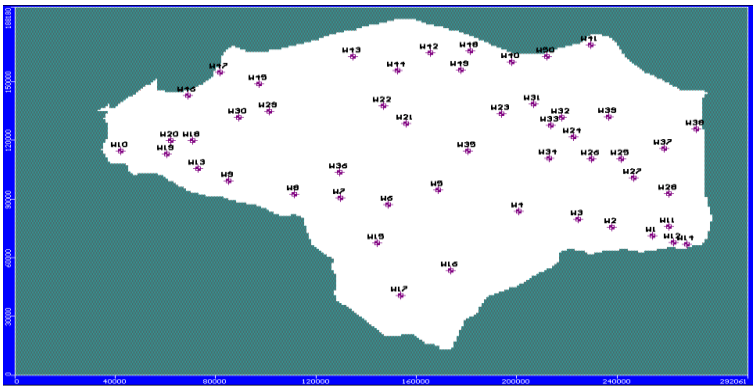

Fig. A8. Calibration point for concentration

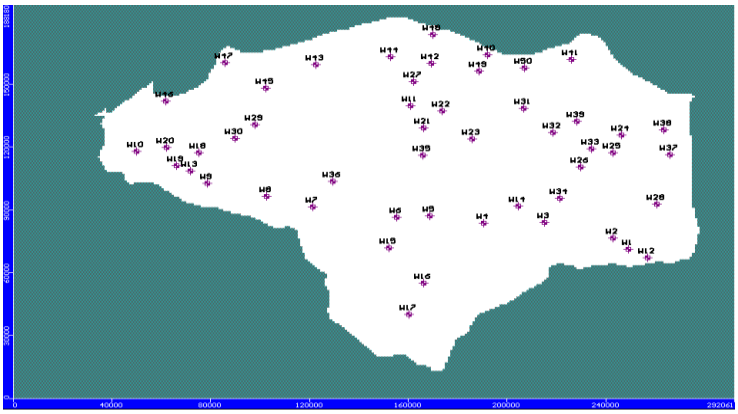

Fig. A9. Validation point for concentration